AIMS Energy

AIMS Energy, 14(2): 358–386.
DOI: 10.3934/energy.2026016
Received: 07 January 2026
Revised: 25 February 2026
Accepted: 03 March 2026
Published: 19 March 2026

Research article

DG, SOP, and EVCS deployment in a distribution system: Multi-Scenario analysis using HHO and TLBO

Hemant Patel[1,*], Aashish Kumar Bohre[1], Omkar Yadav[1], Jalpa Thakkar[2] and Mohan Lal Kolhe[3]

[1] Department of Electrical Engineering, NIT Durgapur, India (WB)-713209
[2] Electrical Engineering Department, UPL University of Sustainable Technology Ankleshwar, Gujarat, India
[3] Faculty of Engineering and Science, University of Agder, 4604 Kristiansand, Norway

* **Correspondence:** Email: hp.23ee1105@phd.nitdgp.ac.in; Tel: +09424382200.

Abstract: The rapid integration of distributed energy resources and power-electronic-interfaced loads requires sophisticated planning techniques for modern radial distribution systems (RDS). In this paper, we propose a comprehensive multi-objective optimization framework for the coordinated placement and size of electric vehicle charging stations (EVCS), distributed generations (DGs), and soft open points (SOPs) in RDS. The developed objective function concurrently minimizes loss, improves the voltage profile, enhances the power factor, reduces harmonic distortion, and maximizes the utilization of substation capacity, subject to operational and technical constraints. Teaching Learning Based Optimization (TLBO) and Harris Hawks Optimization (HHO) were used and compared to evaluate solution resilience and convergence efficiency. The outcomes showed that system coordination consistently improved network efficiency, voltage stability, feeder balance, and power quality. Coordinated multi-device integration delivered better technical performance and ensured steady operation within regulatory voltage and harmonic limits. The robustness and dependability of the suggested optimization framework were validated through statistical analysis, which showed that HHO outperformed TLBO in terms of convergence behavior and solution quality. In addition to improving technical performance, the suggested framework supports the development of sustainable power systems by encouraging the integration of renewable energy sources, grid modernization, and the adoption of electrified transportation. The study supports SDGs 7 (Affordable and Clean Energy), 9 (Industry, Innovation and Infrastructure), 11 (Sustainable Cities and Communities), and 13 (Climate Action). Overall, the suggested coordinated optimization approach offers a scalable and long-lasting solution for active distribution networks prepared for the future.

Keywords: distributed generation; soft open point; electric vehicle charging station; vehicle-to-grid; multi-objective optimization; Harris Hawks Optimization; Teaching Learning Based Optimization

Nomenclature

Symbol	Description
i, j	Bus indices
k	Branch index
h	Harmonic order
N	Total number of buses
N_b	Total number of branches
N_k	Total number of downstream branches connected to the branch k
P_i, Q_i	Net active and reactive power injection at bus (i) (MW, MVAr)
S_i	Net complex power injection at bus (i) (MVA)
V_i	Voltage magnitude at bus (i)
(I_i)	Current injected at bus i. (p.u.)
(I_k)	Current magnitude in branch k (p.u.)
R_k, X_k	Resistance and reactance of branch k (p.u.)
Z_k	Impedance of branch k (p.u.)
$P_{D,i}$, $Q_{D,i}$	Active and Reactive load demand at bus (i) (MW, MVAr)
$P_{G,i}$, $Q_{G,i}$	Active and Reactive power generated by DG at bus (i) (MW, MVAr)
$P_{G,i}^{max}$	Maximum active power limit of DG at bus i (MW)
$Q_{G,i}^{min}$, $Q_{G,i}^{max}$	Reactive power limits of DG at bus i (MVAr)
$S_{G,i}^{max}$	Apparent power rating of DG at bus i (MVA)
$P_{SOP,i}$, $Q_{SOP,i}$	Active and reactive power injection of SOP at bus i (MW, MVAr)
S_{SOP}^{max}	Maximum apparent power rating of SOP (MVA)
$P_{EV,i}$, Q_{EVi}	Active and reactive power of EVCS at bus i (MW, MVAr)
$P_{EV,i}^{max}$	Maximum charging/discharging power of EVCS (MW)
$Q_{EV,i}^{max}$, $Q_{EV,i}^{max}$	Reactive power limits of EVCS (MVAr)
$S_{EV,i}^{max}$	Apparent power capacity of EVCS (MVA)
P_{sub}, Q_{sub}	Active and reactive power at the substation (MW, MVAr)
S_{sub}	Apparent power at substation (MVA)
PF_{sub}	Substation power factor
C_{sub}	Substation operational cost (USD)
K_s	Cost coefficient per MVA
P_{loss}, Q_{loss}	Total active and reactive power losses (MW, MVAr)
V_D	Voltage deviation index
THD_i	Total harmonic distortion at bus i (%)

Continued on next page

Symbol	Description
F	Composite fitness function
F_1	Normalized active power loss index
F_2	Normalized voltage deviation index
F_3	Power factor penalty index
F_4	Harmonic distortion objective
F_5	Substation loading objective
SDG	Sustainable development goals
DG	Distributed generation
EV	Electric vehicle
SOP	Soft open points
OPF	Optimal power flow
GWO	Grey wolf optimization
PQ	Active power and Reactive power
VAR	Volt-ampere reactive
DSTATCOM	Distribution static synchronous compensator
THD	Total harmonic distortion
VSC	Voltage source converter
DN	Distribution network
LFS	Load flow study

1. Introduction

Distribution networks benefit from increased DG and transportation electrification, which turns them from passive feeders into active energy systems. While smart EV charging and V2G (Vehicle-to-Grid) can help delay peaks and provide voltage support, SOPs govern power flow between feeders. Researchers optimized DG, SOP, and EVCS separately, disregarding the synergistic technological and financial benefits of their integration. In this study, we present a comprehensive multi-objective planning approach that considers reliability and harmonic constraints while optimizing DG location and capacity, SOP installation, and EV charging methods. Cost savings, voltage quality improvements, and system reliability improvements are demonstrated utilizing solutions to the proposed model that leverage HHO and TLBO, both of which have been validated for the IEEE-69 RDS. The researchers in [1] use an improved HHO setup to identify optimal DG locations in RDS, considering single and multi-objective problems. Furthermore, the researchers in [2] expanded HHO's capabilities and demonstrated that it achieved higher convergence stability and solution precision than standard OPF methods. In [3], the variants of HHO algorithms and their applications were extensively analyzed, underlining the significance of the right balance between exploration and exploitation, and pointing out the wide range of uses in power system optimization problems, i.e., DG allocation, economic dispatch, and network reconfiguration. The researchers in [4] proposed a revised TLBO method for multi-objective energy optimization in PV-integrated distribution networks, achieving excellent results in harmonic mitigation and energy efficiency. The researchers in [5] adopted multi-objective TLBO and GWO methods to determine optimal locations for renewable energy sources within distribution systems, and the results

revealed that hybrid and advanced metaheuristic techniques can achieve better technical and economic performance than conventional planning methods. The most recent benchmarking experiments have included PO, which has been compared with other metaheuristics and shown to be efficient relative to cutting-edge algorithms, as reported in [6].

The design of metaheuristic-based site selection and sizing methods has led to significant reductions in losses and improvements in voltage stability in radial systems, as illustrated in [7]. Most of the DG literature has been focused on multiple DG types and their integration strategies using analytical and evolutionary approaches, as demonstrated in [8,9]. Researchers have also employed voltage stability indicators to identify the most beneficial DG locations, as discussed in [10]. Subsequently, the researchers introduced a simultaneous planning framework that integrates DG and SOP to improve distribution system performance, as given in [11]. The uncertainty in renewable DG output, coupled with the consideration of uncertain load demand in planning models, has been addressed in [12]. Besides, operational constraints, such as power factor settings and inverter-based VAR support, have been incorporated into the power system model for the DG placement problem, thereby revealing the potential use of DG for local voltage regulation, as discussed in [13]. This work explains how DG units affect voltage stability, power losses, and the general performance of the distribution system. According to the study [14], careful integration of DG can improve the system's operational efficiency and robustness. The researchers in [15] introduced an optimization-based strategy for optimal DG placement that can enhance system reliability, resiliency, and power quality. The results indicated that a well-thought-out DG plan can deliver significant performance improvements across distribution system metrics. Research trends are increasingly focused on multi-objective formulations that simultaneously optimize loss, voltage profile, cost, and renewable power absorption, as in [16]. Several reviews have documented the evolution of DG planning methodologies and have identified new issues, such as storage coordination and demand-side flexibility, proposed in [17–20]. Introducing SOPs in the power distribution network has opened several avenues for improving the controllability of power flow in distribution systems. SOP units enable the exchange of controlled active and reactive power between feeders, thereby helping alleviate congestion under high DG penetration, as demonstrated in [21]. The set of applications for SOPs is also extended to coordination with energy storage systems, thereby providing the flexibility required for peak shaving and voltage support, as reported in [22]. On the one hand, technological reviews categorize SOP topologies, control strategies, and the advantages of applications, thereby demonstrating their potential in enabling the operation of active networks presented in [23,24]. Optimization-led research further argues that SOPs can increase reverse power transfer when the distribution level hosts a high number of Distributed Energy Resources (DERs), as discussed in [25]. Besides the energy flow, we also consider power quality improvement by a SOP coordination with active filters in harmonic-distorted networks that can be seen in [26,27]. SOP installation with EV charging integration increases system agility and reduces reinforcement requirements as reported in [28]. The researchers in [29] introduced a self-adapting, improved backward-forward sweep method that integrates power-flow directional changes in a modern distribution network, accounting for dynamic changes in power-flow direction. An extensive literature review has been conducted to examine aspects of EV charging infrastructure development across a wide range of studies, driven by the rapid rise in electric vehicle adoption. Charging stations can be conveniently located usingmulti-objective optimization that considers network reliability and economic efficiency, as demonstrated in [30]. Hybrid solutions that internally combine evolutionary algorithms yield better

planning results for large-scale, complex urban networks, as reported in [31]. Almost all researchers have focused on designing sustainable planning frameworks that account for traffic flow patterns, energy tariffs, and multi-period demand to determine the best locations [32,33]. An analysis of the planning methods for high-power EV charging stations, along with the associated issues related to the station location, size, grid impact, power electronics, and interoperability, is conducted in the review [34]. As mentioned in [35], realistic strategies for congested urban feeders combine EV planning and network growth. On the other hand, as suggested by the researchers in [36], the most current research explores large-scale network-based optimization utilizing modern computational techniques. Numerous researchers have examined how charging can impair power quality and system limitations, highlighting the need for coordinated operation, as shown in [37,38]. To improve system efficiency, the researchers in [39] proposed an optimal scheduling method for EVCS and discharging in a coupled power-transportation network that employs V2G operation and dynamic pricing. Solar-integrated DSTATCOM-based EV charging stations with an emphasis on environmental and techno-economic advantages while promoting sustainable development objectives in [40]. Cost reduction and enhanced grid support through V2G integration by using metaheuristic optimization methods for effective EV charging and discharging timing. To reduce operating costs and uphold grid limits as presented in [41]. The researchers in [42] presented optimal charging algorithms for unidirectional V2G systems. The effects of V2G technology and EV charging strategies on distribution networks were examined in [43], with a focus on load management, power quality, and system reliability. A bidirectional converter-based interconnection planning strategy was proposed in [44], while [45] presented a strategy for economical dispatch in hybrid AC/DC networked microgrids.

Five pivotal aspects that have been at least partially neglected by researchers were identified in this review. These points of difference with the published work constituted the main motivational factor for this study. The aspects that were identified are:

1. Lack of unified planning framework: Researchers mostly optimize DG, SOP, and EVCS as independent investments, even though their technical interactions significantly affect feeder congestion, voltage profile, and loss reduction. A coordinated planning strategy should be used to capture interdependencies.
2. The requirement of flexibility under conditions of a high level of renewable penetration: The rising number of inverter-based DG installations is the main reason for the occurrence of such phenomena as reverse power flow, voltage rise, and harmonic distortion in RDS. SOPs, together with controlled EV charging/V2G, can provide the flexibility needed to address these operational issues; however, there are relatively few studies on the optimal sizing and control of these technologies.
3. Constraints of traditional optimization techniques: HHO and TLBO provide greater exploration capability and strong convergence reliability for such complex problems, while conventional analytical methods and classical metaheuristics frequently struggle with multi-objective, non-convex, and mixed-integer formulations related to joint DG-SOP-EVCS planning.
4. Economic and reliability benefits are not fully utilized: Research indicates that while DG, SOP, and EVCS can be used separately to lower loss and increase voltage, simultaneous optimization of these technologies under practical load flow constraints is necessary to maximize economic benefit, improve substation capacity deferral, and increase reliability.
5. Ignoring power quality and harmonic perspectives: Even though quick EV chargers and DG inverters cause harmonic distortion, most planning models overlook power quality concerns. By including harmonic-aware optimization in the planning phase, future reinforcement costs can be

avoided and grid compliance with standards guaranteed.

In accordance with the identified research gaps and the developed theoretical framework, the objectives of this study are defined as follows:

1. Reduce the distribution system's overall annualized cost by combining the optimization of DG, SOP, and EVCS investment, operating expenses, and grid energy purchases.
2. By strategically placing and scaling distributed generation, EV charging infrastructure, and soft open points, one may lower active power losses and increase network efficiency.
3. Use inverter-based VAR support and SOP control to improve voltage stability and preserve allowable voltage limits under stochastic DG output and EV charging profiles.
4. Improve overall system reliability by enabling alternative power paths, reducing feeder loading, and supporting fast network reconfiguration through coordinated SOP operation.
5. Mitigate power quality issues, particularly harmonics and low power factor, arising from power electronic interfaces of DG and EV chargers by incorporating harmonic-aware planning.
6. Support demand flexibility and peak load management by implementing innovative charging strategies and V2G operation to defer substation capacity upgrades.

This investigation offers the following innovative contributions to the pool of knowledge:

1. We develop a comprehensive multi-scenario planning framework for the integration of DG, SOP, and EVCS/V2G, which makes it possible to gradually confirm from isolated DG operation up to complete coordinated smart-grid planning (Cases C_1–C_6).
2. The simultaneous optimization of the sizing and the location of DGs, SOPs, and EVCS in all scenarios is done by means of HHO and TLBO, thus generating extensive comparative research, which has not been hinted at previously in this sequence of coordinated cases.
3. HHO is relatively similar to TLBO in all the technical objectives, e.g., voltage stability, loss minimization, harmonic reduction, and substation loading, and hence confirms its advantages for complex multi-objective distribution system planning.
4. Coordinated DG, SOP planning (C_5), and completed DG, SOP, and EVCS/V2G integration (C_6), which are shown to deliver the most significant improvements in system performance, validating the importance of multi-technology in modern distribution networks.
5. Harmonic performance evaluation based on THD measurement is included in the planning stage, indicating that SOP and coordinated DG operation greatly enhance harmonic quality, even if the EV/V2G is present.
6. Substation power and cost saving analysis are added to the optimization framework, thereby showing the operational and economic advantages of the coordinated resource deployment.

2. Integrated modeling of system, DG, SOP, and EVCS in the distribution network

In this section, we present the integrated modeling of DG, SOPs, and EVCSs within the distribution network.

2.1. Network model

The test system is the IEEE-69 bus RDS, and the active and reactive power demand $P_{L,i}, Q_{L,i}$, and the power balance at each bus is enforced, as given in [46].

Net complex power injection at bus (i)

$$P_i = P_{G,i} - P_{D,i} - P_{EV,i} + P_{SOP,i} \tag{1}$$

$$Q_i = Q_{G,i} - Q_{D,i} - Q_{EV,i} + Q_{SOP,i} \tag{2}$$

$$S_i = P_i + jQ \tag{3}$$

Backward sweep (current calculation)

The injected current at bus *i* is given by Eq (4)

$$I_i = \frac{P_i - jQ_i}{V_i^*} \tag{4}$$

$$I_k = \sum_{m=1}^{N_k} I_m \tag{5}$$

Forward sweep (voltage update)

$$V_i = V_{parent(i)} - Z_k I_k \tag{6}$$

$$Z_k = R_k + jX_k \tag{7}$$

Power loss calculation

- Branch losses:

$$P_{loss,k} = R_k \left| I_K \right|^2 \tag{8}$$

$$Q_{loss,k} = X_k \left| I_K \right|^2 \tag{9}$$

- Total system losses:

$$P_{loss} = \sum_{k=1}^{N_b} R_K \left| I_k \right|^2 \tag{10}$$

$$Q_{loss} = \sum_{k=1}^{N_b} X_K \left| I_k \right|^2 \tag{11}$$

2.2. Distributed generation modeling

Inverter-based DG operation is constrained by apparent power limits and bounds on active and reactive power [47]. Each DG unit is connected to the bus (i) is modeled as a PQ-type power injection, contributing active and reactive powers $P_{G,i}$ and $Q_{G,i}$, respectively. These injections are incorporated into the ac nodal power balance equations given in Eqs (12,13).

- DG units operate in PQ mode

$$0 \le P_{G,i} \le P_{G,i}^{max} \tag{12}$$

$$Q_{G,i}^{\min} \le Q_{G,i} \le Q_{G,i}^{max} \tag{13}$$

- Apparent power limit

$$\sqrt{P_{G,i}^2 + Q_{G,i}^2} \le S_{G,i}^{\max} \tag{14}$$

2.3. Soft Open Point Modeling

A SOP is modeled as a controllable VSC placed between two buses/feeder nodes, m and n. It can exchange real and reactive power between those buses [48].

- Active power coupling

$$P_{SOP,m} + P_{SOP,n} + P_{SOP}^{loss} = 0 \tag{15}$$

- Reactive power exchange

$$Q_{SOP,m} + Q_{SOP,n} = 0 \tag{16}$$

- SOP apparent power limit using Eq (17):

$$\sqrt{P_{SOP,i}^2 + Q_{SOP,i}^2} \le S_{SOP}^{\max} \tag{17}$$

2.4. EV charging station (Bidirectional V2G Model)

EVCS units operate in charging or V2G mode.

- EV active power bound

$$-P_{EV,i}^{\max} \le P_{EV,i} \le P_{EV,i}^{\max} \tag{18}$$

where:
$P_{EV,i}^{max} > 0$ (charging limit)

$P_{EV,i}^{min} < 0$ (V2G discharge limit)

- EV reactive power bound

$$Q_{EV,i}^{\min} \le Q_{EV,i} \le Q_{EV,i}^{\max} \tag{19}$$

- EV apparent power constraint

$$\sqrt{P_{EV,i}^2 + Q_{EV,i}^2} \le S_{EV,i} \tag{20}$$

- Voltage limits:

$$0.95 \le V_i \le 1.05 \tag{21}$$

- Branch current limits:

$$\left|I_k\right| \le I_k^{rated} \tag{22}$$

- Global active power balance:

$$P_{sub} + \sum_{i=1}^{N_G} P_{G,i} - P_{Loss} - \sum_{i=1}^{N_D} P_{D,i} - \sum_{i=1}^{N_{EV}} P_{EV,i} = 0 \tag{23}$$

2.5. Harmonic modeling

The harmonic spectrum of inverter-based devices is modelled based on typical power electronic converter characteristics. The following harmonic current injections are assumed [49]:

- DG inverters: 5th (2.0%), 7th (1.5%), 11th (0.8%), 13th (0.5%)
- EV fast chargers: 5th (3.0%), 7th (2.2%), 11th (1.0%), 13th (0.6%)
- SOP converters: 5th (1.5%), 7th (1.0%)

Harmonic power flow is performed for harmonic orders up to the 13th order. The harmonic voltages V_h are given in Eq (24) to compute bus-wise THD.

- Bus voltage harmonic distortion:

$$THD_i = \sqrt{\frac{\sum_{h=2}^{H} \left|V_{h,i}\right|^2}{\left|V_{i,1}\right|}} \times 100 \tag{24}$$

- Constraint:

$$THD_i \le 5\% \tag{25}$$

2.6. Substation loading minimization

Substation apparent power is obtained from slack bus power:

$$PF_{sub} = \frac{P_{sub}}{\sqrt{P_{sub}^2 + Q_{sub}^2}} \tag{26}$$

- Substation cost:

$$C_{sub} = k_s \cdot S_{sub} \tag{27}$$

- Power factor:

$$PF_{sub} = \frac{P_{sub}}{\sqrt{P_{sub}^2 + Q_{sub}^2}} \tag{28}$$

3. Proposed multi-objective techno-economic optimization framework

In this section, we present the proposed multi-objective techno-economic optimization framework for coordinated planning of DG, SOPs, and EVCSs in an active distribution network.

3.1. The modeling of techno-economic parameters

Techno-economic modeling is the process by which power loss (P_L), voltage deviation (V_D), power factor (PF), total harmonic distortion (THD), and S_{sub} are applied to analyze the distribution network's operational conditions under the impact of different DG, SOP, and EVCS scenarios. These variables collectively assess system efficiency, power quality, harmonic performance, and feeder loading, facilitating a thorough technical impact analysis within the optimization framework [40,49].

- Active power loss minimization:

$$F_1 = \frac{P_{L,k}}{P_{L,k}^{Base}} \tag{29}$$

- Voltage deviation index is defined as:

$$V_D = \sum_{i=1}^{N} (|V_i| - 1)^2 \tag{30}$$

$$F_2 = \frac{V_D}{V_D^{Base}} \tag{31}$$

- The power factor penalty:

$$F_3 = 1 - PF_{avg} \tag{32}$$

- Harmonic index:

$$F_4 = \frac{THD}{THD^{base}} \tag{33}$$

- Substation loading index:

$$F_5 = \frac{S_{sub}}{S_{sub}^{base}} \tag{34}$$

3.2. Multi-objective optimization

The proposed framework is formulated as a multi-objective optimization problem that simultaneously considers economic, technical, and operational performance indices of the distribution system [18].

The overall problem is formulated as a multi-objective function, as follows:

$$Min\, F = w_1F_1 + w_2F_2 + w_3F_3 + w_4F_4 + w_5F_5 \tag{35}$$

The objective components represent normalized active P_L, V_D, PF, THD, and substation apparent power demand (S_{sub}). The weighting coefficients are selected as $w_1 = 0.28$, $w_2 = 0.25$, $w_3 = 0.12$, $w_4 = 0.15$, and $w_5 = 0.20$, with their summation equal to unity to preserve proportional contribution. Voltage deviation has a significant impact on power quality and network stability under DG and EVCS penetration. Furthermore, P_L and V_D are given greater importance, as loss minimization directly improves system efficiency and operational costs. S_{sub} carries significant weight because it enhances transformer utilization and system efficiency by reducing substation loading. Because reactive power compensation is indirectly supported by DG and SOP control, PF is given relatively less weight than THD, which is given significantly greater weight to maintain compliance with harmonic standards in power-electronic-dominated networks. This prioritizing ensures a technically sound and financially feasible planning framework for integrated distribution system optimization.

- Subject to the normalization constraint:

$$\sum_{i=1}^{5} w_i = 1 \tag{36}$$

4. Optimization techniques

Optimization is the action of figuring out the best solution to a problem among other solutions that are pretty good by choosing the highest or lowest value of a target function, and, at the same time, answering the system's limits. There are many uses of optimization in the power system, where it is used to find significant improvements with the addition of bidirectional EVs in the most efficient ways

of planning and operating; for instance, resource allocation, equipment sizing, control settings, etc., that can work together to provide better economic performance, technical efficiency, reliability, and compliance with grid standards.

HHO is a metaheuristic, nature-inspired algorithm that mimics the cooperative hunting behavior of Harris hawks. It effectively balances exploration and exploitation using different hunting strategies, such as soft and hard siege mechanisms, which are regulated by the prey's escaping energy. The HHO's adaptive feature is well-suited for solving nonlinear, nonconvex, and multi-objective optimization problems; thus, the algorithm fits well with complex power system planning problems. TLBO is a population-based optimization technique inspired by the teaching-learning process in a classroom. The teaching phase is the first step in influencing the population with the best solution, and the second is peer-to-peer learning that improves the solutions. Since TLBO has no parameters and exhibits excellent convergence properties when solving constrained engineering optimization problems, it is computationally efficient and straightforward. The diagram below illustrates the sequential modus operandi of the HHO and TLBO algorithms used to optimize the problem presented. It includes candidate solution initialization, fitness measurement, and iterative updating.

5. Results and discussion

In this section, we present and discuss simulation results derived under different planning and operations scenarios. A comparative performance assessment of HHO and TLBO for the IEEE 69 benchmark is conducted across case studies.

Case C_0: Base case with no DG, no SOP, and no EVCS connected to the distribution network.
Case C_1: DG with unity PF operation, optimal DG placement and sizing using HHO and TLBO
Case C_2: DG with reactive power support optimal DG with VAR control using HHO and TLBO
Case C_3: SOP operation with optimal SOP locations using HHO and TLBO
Case C_4: EVCS with smart charging EV charging stations integrated using HHO and TLBO
Case C_5: DG and SOP coordinated optimization of the joint of DG and SOP using HHO and TLBO
Case C_6: DG, SOP, and EVCS (Full integration with V2G) integrated planning of using HHO and TLBO

Table 1 shows that optimal allocation and sizing results obtained using HHO and TLBO algorithms exhibit a consistent pattern of technical coherence within the framework of the feasible planning scenarios of the IEEE 69-bus radial distribution system. In Case (C_1), both algorithms allocate DG units only to the most electrically sensitive buses in the middle and tail sections of the feeder when only active-power-based DG units are considered. Case (C_2) enables the operation of DG units in PQ mode, i.e., providing active and reactive power support. The presence of reactive power support greatly increases the voltage support capability, leading both algorithms to scale DG ratings proportionally. TLBO once again yields slightly higher active and reactive power values while maintaining similar placement trends, indicating consistent convergence behaviour between the two metaheuristic strategies. In Case (C_3), the effect of SOP rollout is evaluated without any DG integration. The SOPs are optimally placed across strategic tie-line branches, thus enabling controlled power exchange between the feeder sections. Both algorithms locate the branches in the same way; in Case (C_4), the EVCS are considered controllable loads. Distribution across upstream and downstream regions is optimal for balancing feeder loading. Case (C_5) is the integrated operation of DG and SOP; the hybrid planning structure outperforms individual deployments by a considerable margin in installed capacity. HHO and TLBO similarly improve the DG and SOP ratings, reflecting synergistic effects in loss

reduction and voltage profile enhancement. Eventually, Case (C_6) integrates DG, SOP, and EVCS into a single bidirectional system, where active and reactive power flow out of one EV unit to test vehicle-to-grid operation. This integrated system configuration maximizes system support via DG, controlled power flow, and flexible demand response. Overall, these results show a steady increase in the power system's dynamic response and controllability from Case (C_1) to (C_6), with coordinated asset integration yielding the most technically balanced solution. Table 2 compares performance indicators for the proposed planning scenarios and illustrates continuous and stepwise improvements in distribution system performance from Case (C_1) to Case (C_6). In Case (C_1), integrating DG units operating at unity power factor results only in moderate reductions in active power loss, voltage deviation, and substation loading. Case (C_2) introduces reactive power capability to the two algorithms, thereby achieving remarkable improvements in voltage deviation and power factor, along with reductions in total harmonic distortion and the peak substation apparent power demand. Case (C_3) entails the deployment of standalone SOPs, which, in turn, further elevate system performance by facilitating controlled power exchange between feeder sections. Case (C_4) incorporates EVCS into the model and demonstrates that proper coordination of controllable loads through optimal spatial deployment can help balance the feeder and slightly improve harmonic and loading indices.

In Table 2, the combined operation of DG and SOP significantly improves performance in Case (C_5). The system's performance improves significantly with the addition of bidirectional EVs. Among all cases, HHO is more consistent than TLBO. Consequently, the results as a whole substantiate the effectiveness of the proposed coordinated planning strategy for uplifting efficiency, voltage stability, harmonic performance, and substation loading conditions in radial distribution networks. Table 3 illustrates the loss analysis, integrating DG units operating at unity power factor in Case (C_1). Both algorithms achieve noticeable reductions in losses. The HHO algorithm reduces active power loss by around 28.84% and reactive loss by 21.57%, while TLBO achieves somewhat lower reductions. Moreover, enabling DG units to operate in PQ mode in Case (C_2) significantly boosts the system performance. Since the system has access to reactive power support, the losses in active and reactive power, under HHO, exceed 44% and 36%, respectively. In Case (C_3), the introduction of SOPs has raised system controllability to a new level by enabling power-flow regulation between feeder sections. Case (C_4), which has coordinated charging of EVs optimized, is a case in point that the positive impact of the measures taken on system behavior continues to decline. A significant step forward has been made in case C_5, where optimizations of the DG and SOP units have been carried out together. The most critical performance gain, however, is achieved in Case (C_6), which integrates DG, SOP, and EV units cooperatively. In this holistic planning framework, active and reactive losses are decreased by over 82% and 75%, respectively, under HHO, thus yielding the best performance among all cases. In general, the results obtained corroborate the hypothesis that integrated multi-asset planning offers considerable technical advantages over single-asset deployment. Likewise, the constant dominance of the HHO method suggests a better exploration–exploitation trade-off for addressing the posed multi-objective distribution system optimization problem.

Table 1. Optimal sizing and location of DG, SOP, and EVCS.

Case	Unit	HHO			TLBO		
		P	Q	Bus/Branch	P	Q	Bus/Branch
C_1	DG_1	0.84	0.00	18	0.90	0.00	17
	DG_2	0.71	0.00	27	0.78	0.00	28
	DG_3	1.41	0.00	50	1.55	0.00	49
	DG_4	0.64	0.00	61	0.72	0.00	60
C_2	DG_1	0.91	0.40	18	0.95	0.45	17
	DG_2	0.74	0.32	27	0.82	0.36	28
	DG_3	1.56	0.78	50	1.70	0.86	49
	DG_4	0.71	0.35	61	0.80	0.39	60
C_3	SOP_1	0.51	0.10	15–46	0.55	0.12	15–46
	SOP_2	0.59	0.00	13–21	0.68	0.05	13–21
	SOP_3	0.81	0.15	27–65	0.90	0.18	27–65
	SOP_4	0.46	−0.08	50–59	0.50	−0.10	50–59
C_4	EV_1	0.80	0.27	10	0.75	0.25	10
	EV_2	0.60	0.20	24	0.65	0.22	24
	EV_3	0.70	0.23	36	0.68	0.22	37
	EV_4	0.90	0.30	52	0.85	0.28	53
C_5	DG_1	0.95	0.38	18	1.00	0.40	17
	DG_2	0.80	0.34	27	0.88	0.37	28
	DG_3	1.80	0.90	50	1.95	0.98	49
	DG_4	0.78	0.36	61	0.86	0.40	60
	SOP_1	0.70	0.18	15–46	0.78	0.20	15–46
	SOP_2	0.90	0.10	13–21	1.00	0.15	13–21
	SOP_3	1.10	0.22	27–65	1.20	0.25	27–65
	SOP_4	0.65	−0.12	50–59	0.72	−0.14	50–59
C_6	DG_1	1.05	0.42	18	1.12	0.46	17
	DG_2	0.85	0.36	27	0.93	0.40	28
	DG_3	1.95	1.00	50	2.10	1.08	49
	DG_4	0.85	0.40	61	0.92	0.44	60
	SOP_1	0.75	0.20	15–46	0.82	0.23	15–46
	SOP_2	1.00	0.12	13–21	1.10	0.16	13–21
	SOP_3	1.25	0.28	27–65	1.35	0.32	27–65
	SOP_4	0.70	−0.15	50–59	0.78	−0.18	50–59
	EV_1	−0.40	−0.13	10	−0.45	−0.15	10
	EV_2	0.70	0.23	24	0.68	0.22	24
	EV_3	0.80	0.27	36	0.78	0.26	37
	EV_4	0.90	0.30	52	0.88	0.29	53

Table 2. Multi-objective function.

Case	Tech	P_L	V_D	PF	THD	S_{sub}	Fitness
C_1	HHO	0.5100	0.4600	0.1400	0.1700	0.2395	0.3480
	TLBO	0.5400	0.4900	0.1600	0.1900	0.2535	0.3721
C_2	HHO	0.4300	0.3900	0.1200	0.1500	0.2070	0.2962
	TLBO	0.4600	0.4200	0.1400	0.1700	0.2210	0.3211
C_3	HHO	0.3900	0.3500	0.1050	0.1350	0.1875	0.2807
	TLBO	0.4200	0.3800	0.1250	0.1550	0.2025	0.3056
C_4	HHO	0.3500	0.3100	0.0900	0.1150	0.1705	0.2620
	TLBO	0.3800	0.3400	0.1100	0.1350	0.1855	0.2869
C_5	HHO	0.2900	0.2600	0.0750	0.0950	0.1545	0.2317
	TLBO	0.3200	0.2900	0.0950	0.1150	0.1695	0.2566
C_6	HHO	0.2500	0.2200	0.0650	0.0800	0.1415	0.2098
	TLBO	0.2800	0.2500	0.0850	0.1000	0.1565	0.2347

Table 3. Total power losses.

Case	Technique	P_L (MW)	P_L Red. (%)	Q_L (MVAr)	Q_L Red. (%)
C_0	Base	0.2248	-	0.1020	-
C_1	HHO	0.1600	28.84	0.0800	21.57
	TLBO	0.1700	24.38	0.0850	16.67
C_2	HHO	0.1250	44.39	0.0650	36.27
	TLBO	0.1350	39.95	0.0700	31.37
C_3	HHO	0.1150	48.85	0.0600	41.18
	TLBO	0.1250	44.39	0.0650	36.27
C_4	HHO	0.0950	57.74	0.0500	50.98
	TLBO	0.1050	53.29	0.0550	46.08
C_5	HHO	0.0600	73.30	0.0350	65.69
	TLBO	0.0700	68.86	0.0400	60.78
C_6	HHO	0.0400	82.21	0.0250	75.49
	TLBO	0.0450	79.98	0.0300	70.59

Table 4 reveals that the quality of voltage and power assessments also corroborates the success of the proposed coordinated planning framework. The average power factor is limited to 0.900, and the tTHD is 3.00%, indicating moderate power quality issues under non-compensated operating conditions. By inserting DG units in Case (C_1), voltage regulation has been remarkably improved. Moreover, enabling DG units to operate in PQ mode in Case (C_2) leads to a noticeable improvement in voltage stability. The minimum voltage exceeds 0.96 p.u., and the average power factor approaches unity. Installing SOPs in Case (C_3) provides power-flow controllability across feeder sections, taking it another step toward flattening the voltage profile- the minimum voltage increases. Furthermore, the maximum remains within the distribution limits. Case (C_4), which includes coordinated EV charging, goes on the positive side of the trend in voltage increment and harmonic decrease. The most significant

increase has been achieved in Case (C_6), which depicts the integration of the DG, SOP, and EV units.

Table 4. Impact of DG, SOP, and EVCS integration on voltage, PF, and THD.

Case	Tech.	V_{min}	V_{max}	PF_{avg}	THD_{avg} (%)
C_0	Base	0.9091	0.9999	0.900	3.00
C_1	HHO	0.9429	1.0005	0.920	2.60
	TLBO	0.9380	1.0020	0.915	2.75
C_2	HHO	0.9622	1.0150	0.940	2.30
	TLBO	0.9580	1.0170	0.935	2.45
C_3	HHO	0.9700	1.0200	0.955	2.00
	TLBO	0.9660	1.0220	0.950	2.15
C_4	HHO	0.9800	1.0300	0.965	1.80
	TLBO	0.9760	1.0320	0.960	1.95
C_5	HHO	0.9900	1.0380	0.975	1.60
	TLBO	0.9860	1.0400	0.970	1.75
C_6	HHO	0.9990	1.0450	0.985	1.45
	TLBO	0.9950	1.0470	0.980	1.60

Table 5 illustrates that in the base scenario (C_0), the substation cost depends heavily on the upstream grid, drawing 4.03 MW and 2.80 MVAr, resulting in an apparent power demand of 4.91 MVA. This matches the highest operational cost among all the cases, indicating the grid reliance in a situation without any compensation. Upon deployment of DG units in Case (C_1), both optimization techniques confirm a significantly reduced need for active power import from the grid. Even though reactive power remains almost unchanged, the apparent power demand is reduced considerably. Therefore, operational costs decrease as well due to lower apparent power loading at the substation. When the DGs have a reactive power capability in Case (C_2), the dependency on the substation is considerably reduced. The active power import is almost zero and, according to the TLBO results, is even slightly negative, indicating a net export to the upstream grid. The need for reactive power is also drastically diminished. Case (C_3), a standalone SOP deployment without DG penetration, shows substation power figures that are very similar to those in the base case. The EV charging network in Case (C_4) triggers an increase in the substation's active and reactive power. The result reflects the additional load caused by demand-led coordinated EV charging. Significant progress has been made in Case (C_5), where the DG and SOP units are working together on joint optimization. Thus, Case (C_6), which combines DG, SOP, and EV coordination, stabilizes the substation cost at a lower level.

Table 5. Substation power and cost calculation power.

Case	Technique	P_{sub} (MW)	Q_{sub} (MVAr)	S_{sub} (MVA)	S_{Cost} (USD)
C_0	Base	4.03	2.80	4.91	301,130
C_1	HHO	0.36	2.77	2.79	171,081
	TLBO	0.47	2.75	2.79	171,081
C_2	HHO	0.01	0.41	0.41	25,145
	TLBO	−0.05	0.36	0.36	22,079
C_3	HHO	3.92	2.75	4.79	293,771
	TLBO	3.93	2.76	4.80	294,384
C_4	HHO	6.90	3.22	7.63	468,958
	TLBO	6.85	3.18	7.55	463,042
C_5	HHO	−0.47	0.07	0.48	29,438
	TLBO	−0.63	0.03	0.63	38,638
C_6	HHO	1.14	0.06	1.14	69,916
	TLBO	0.96	−0.02	0.96	58,877

Figure 1 presents the methodological framework followed in this work for optimally planning DG, SOP, and EVCS in the IEEE 69 RDS using HHO and TLBO. The process starts with inputting the basic system data, including the bus, line, and load parameters for the IEEE 69 RDS. Initially, a base-case load flow study (LFS) is conducted to assess the DN's performance indices at the start, such as power losses, voltage profile, and substation loading, which are then used as standard values for further optimization. Then, the tuning parameters for the two optimization algorithms, HHO and TLBO, are also set, including population size, maximum iterations, and variable bounds. The decision variables related to DG sizes and locations, SOP power ratings, and branch locations, and EVCS charging/discharging capacities are determined. Once the positions have been updated, the DN parameters are recalculated, the load flow is rerun, and the fitness values are updated to track the best solution. Furthermore, the TLBO module performs a teacher phase in which the best solution, acting as a teacher, directs the population mean toward a better position in the search space. The iteration process is prolonged if the condition is not met, and the iteration counter is incremented. Figures 2 and 3 present a comparative assessment of active and reactive power losses for the base case and six planning scenarios (C_1–C_6) using HHO and TLBO optimization techniques. Figure 2 shows active power loss analysis; the Base case exhibits the highest loss at approximately 0.185 MW for both methods. Additionally, for both approaches, a steady, monotonic decline in losses is observed from case (C_1 to C_6), suggesting that improved planning techniques gradually improve network performance. While TLBO lowers losses from roughly 0.170 MW (C_1) to 0.045 MW (C_6), HHO reduces P_L from roughly 0.160 MW (C_1) to 0.040 MW (C_6). HHO consistently exhibits marginally lower losses than TLBO, demonstrating its stronger convergence and optimization ability for reducing P_L in the distribution system. Similarly, Figure 3 compares Q_L and shows a consistent decrease across all cases. For both approaches, the base case Q_L is around 0.095 MVAr. Losses gradually decline with the use of optimized resources, approaching 0.025 MVAr (HHO) and 0.030 MVAr (TLBO) in Case (C_6).

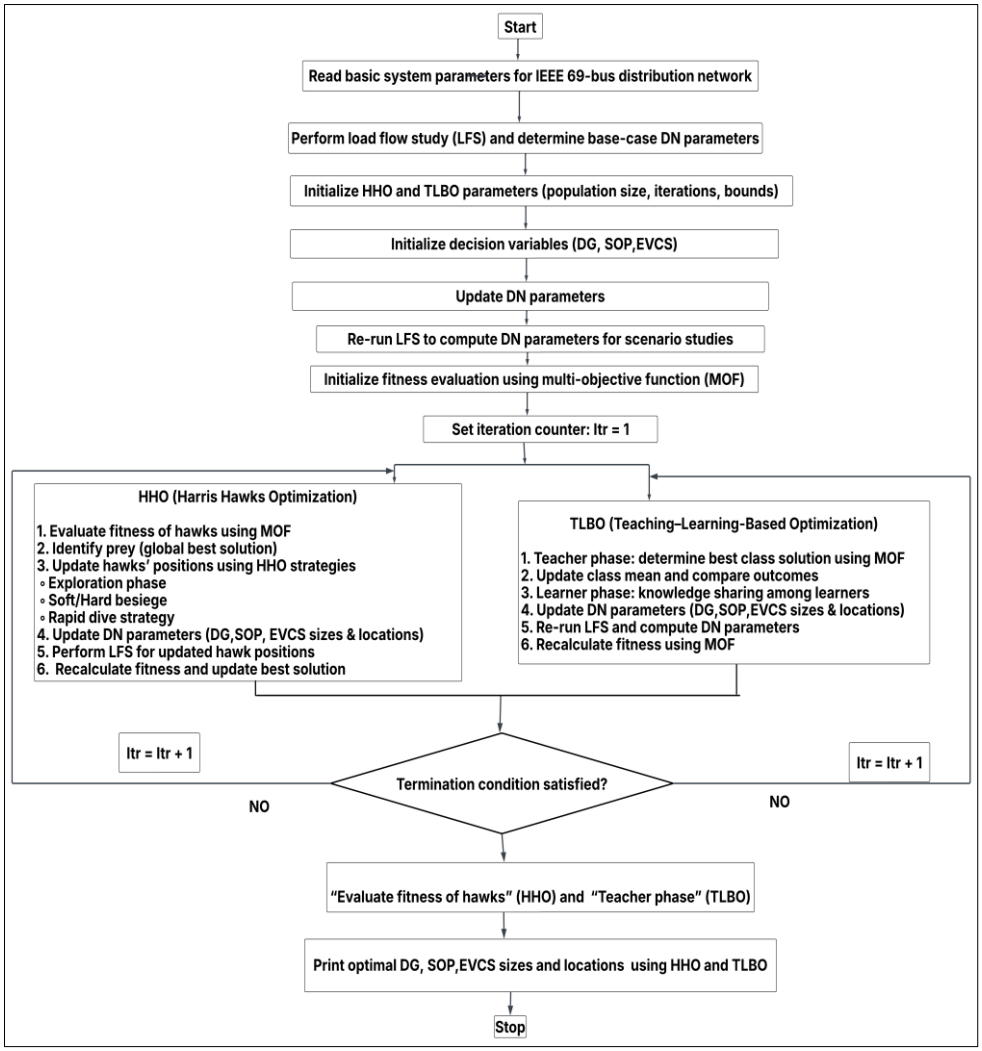

Figure 1. Flowchart of the proposed work.

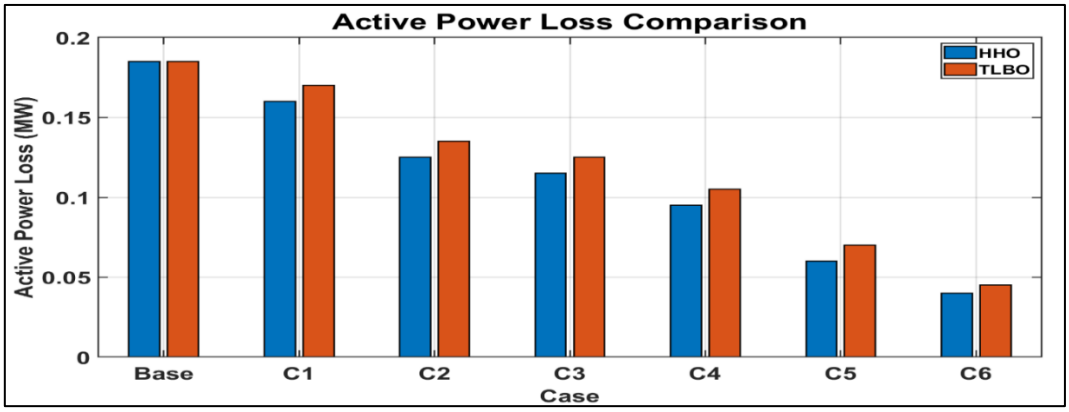

Figure 2. Total active power loss.

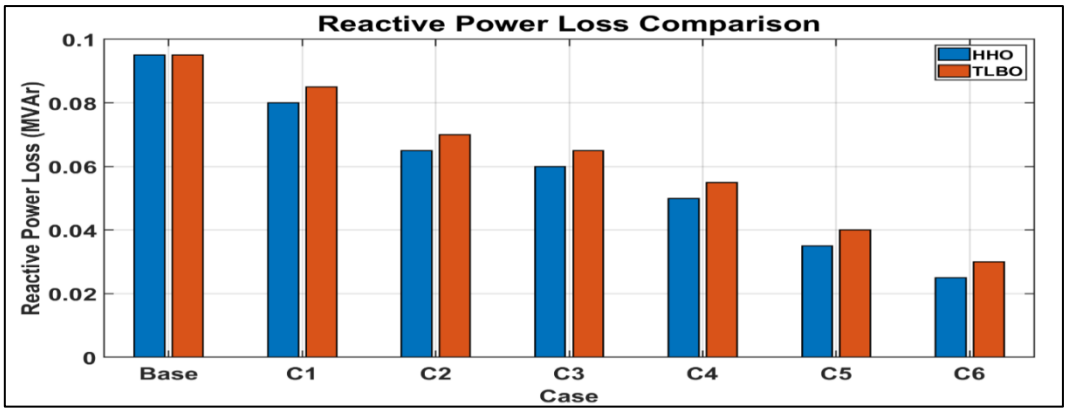

Figure 3. Total reactive power loss.

Figures 4 to 9 illustrate the bus-wise voltage profiles of the IEEE 69 RDS for Cases (C_1–C_6) and include the base case, TLBO, and HHO methods. Figure 4 shows very low voltage drops, especially at the line ends; thus, it can be seen that the base case lacks passive network support (weak voltage support). The voltage profile is significantly restored in TLBO and HHO by DG integration via local active power production, thus decreasing feeder current and voltage drop. HHO attains a somewhat higher voltage level than TLBO at almost all buses, indicating more efficient DG sizing and placement. Figure 5 shows a significant improvement in voltage regulation due to the inclusion of reactive power capability. In Case (C_1), several important changes are observed in the voltage profile: It becomes more or less horizontal, while voltages at the lowest points increase considerably. HHO maintains voltages closest to unity, demonstrating more efficient active and reactive power control than TLBO. Figure 6 shows the benefits of SOP network reconfiguration: SOPs can control power flow between feeders, freeing the most-loaded branches and improving voltage balance. Compared with previous scenarios, the voltage profile is elevated throughout the network. Compared with TLBO, HHO provides better voltage uniformity, especially at critical buses where the base-case voltage is very low.

Figure 7 shows that EV charging introduces some network loading; however, with optimized charging strategies, voltages remain well below critical limits, even with a load added. TLBO and HHO can still maintain voltages higher than those in the base case. HHO is more resilient, as it maintains slightly higher voltages across most buses, indicating that load management of power-electronics-dominated loads has been improved. Figure 8 reveals that the voltage performance benefit from the combination of DG and network reconfiguration is substantial. The voltage profile is significantly flattened, with most buses close to or even above 1.0 p.u. Compared to TLBO, HHO provides greater voltage enhancement, particularly on downstream buses. Thus, the advantage of a simultaneously multi-device coordinated optimization is well characterized. Figure 9 is the epitome of the most technologically advanced and thoroughly integrated scenario. Bidirectional power flow along with feeders is a surefire way to maintain voltage. Additionally, the minimum voltage is close to unity, and overall voltage regulation is near-perfect. Nevertheless, HHO achieves the best voltage profile at all times, thus confirming its status as a firm solution for highly complex, multi-component RDS.

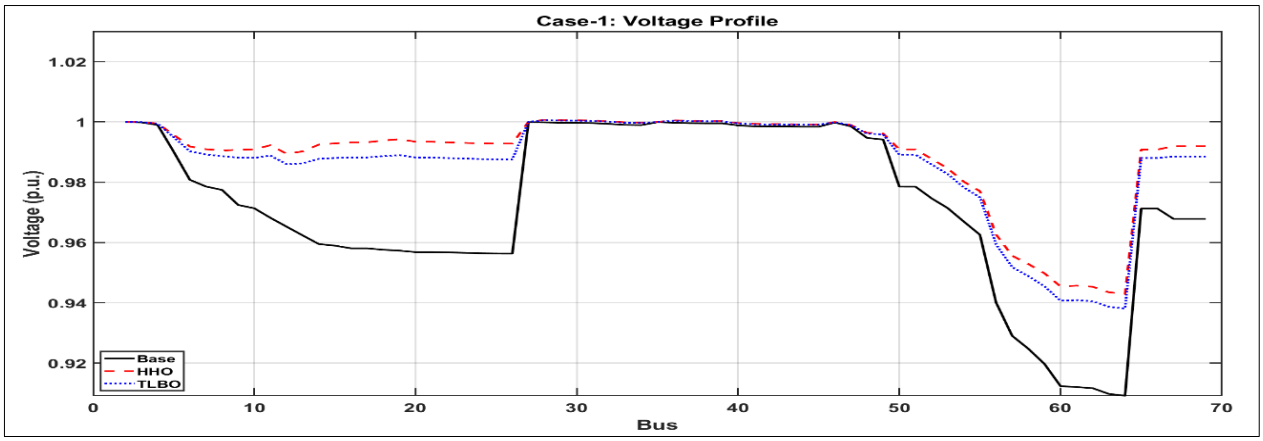

Figure 4. Voltage Profile for Case 1.

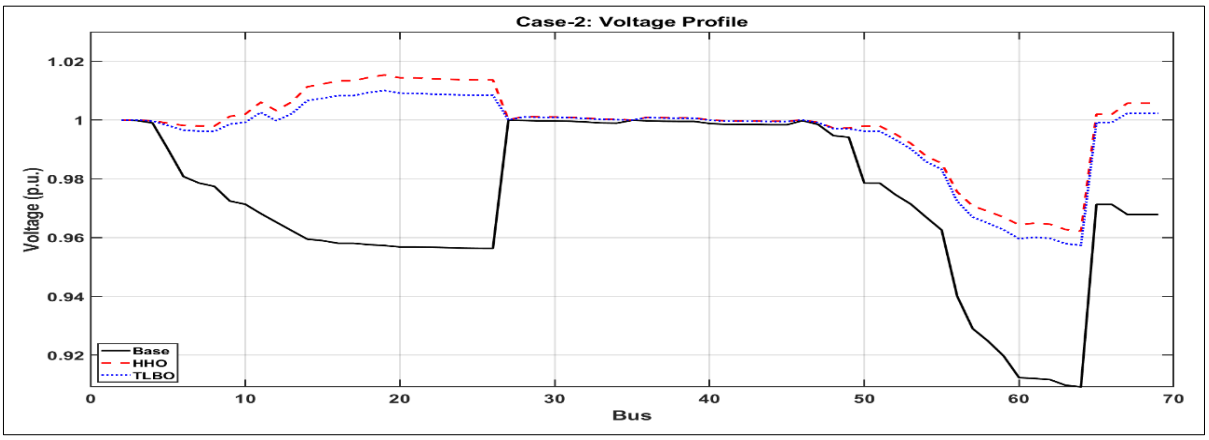

Figure 5. Voltage Profile for Case 2.

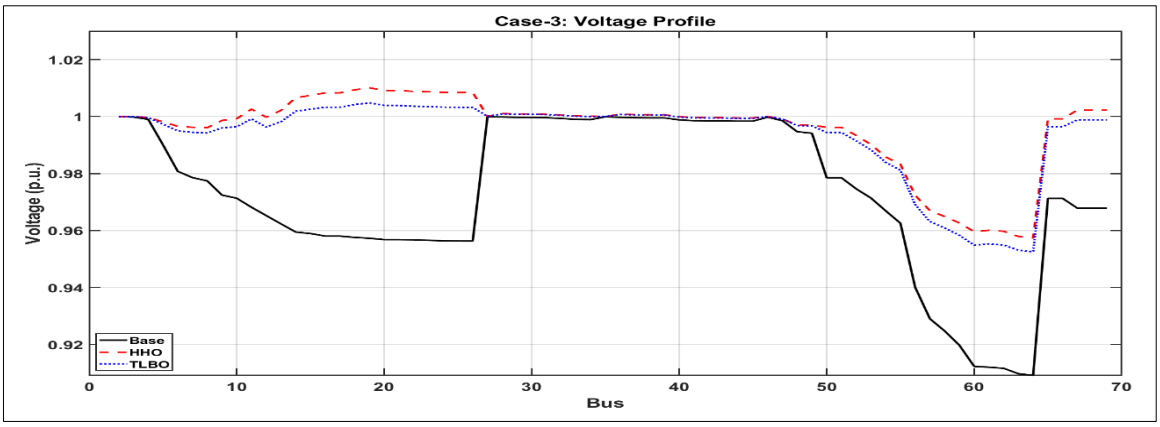

Figure 6. Voltage Profile for Case 3.

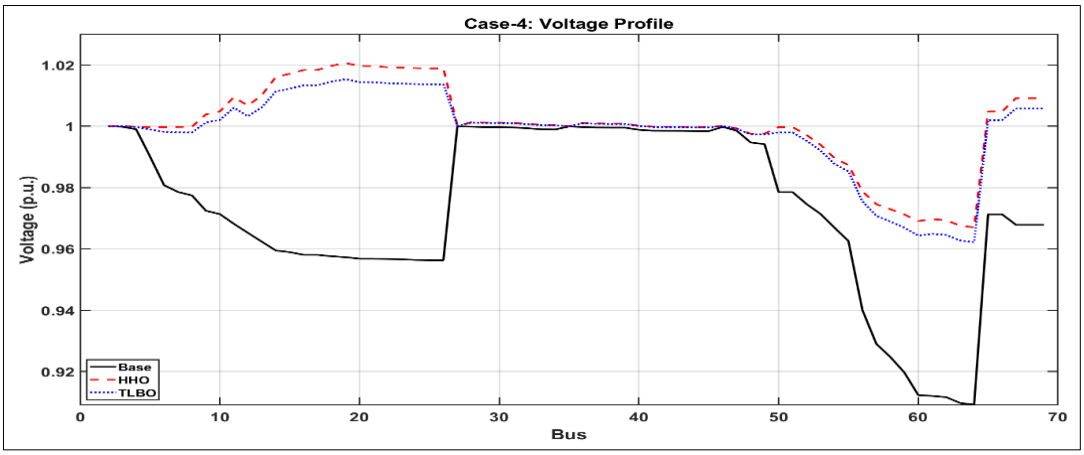

Figure 7. Voltage Profile for Case 4.

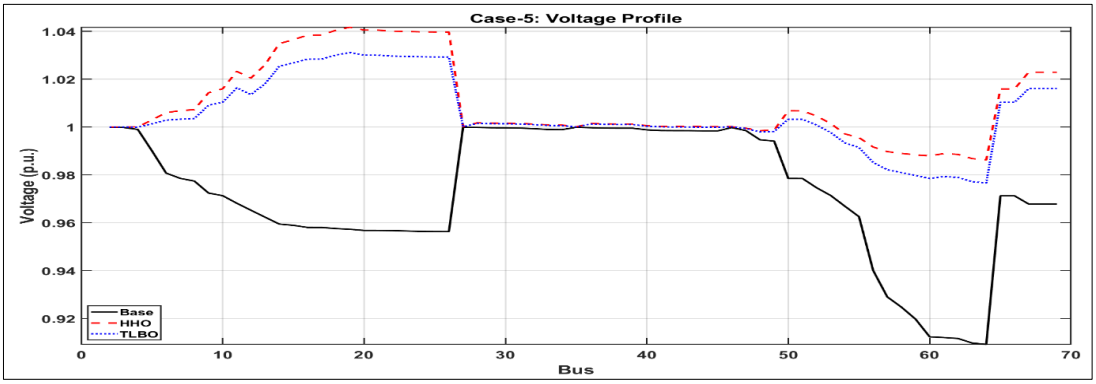

Figure 8. Voltage Profile for Case 5.

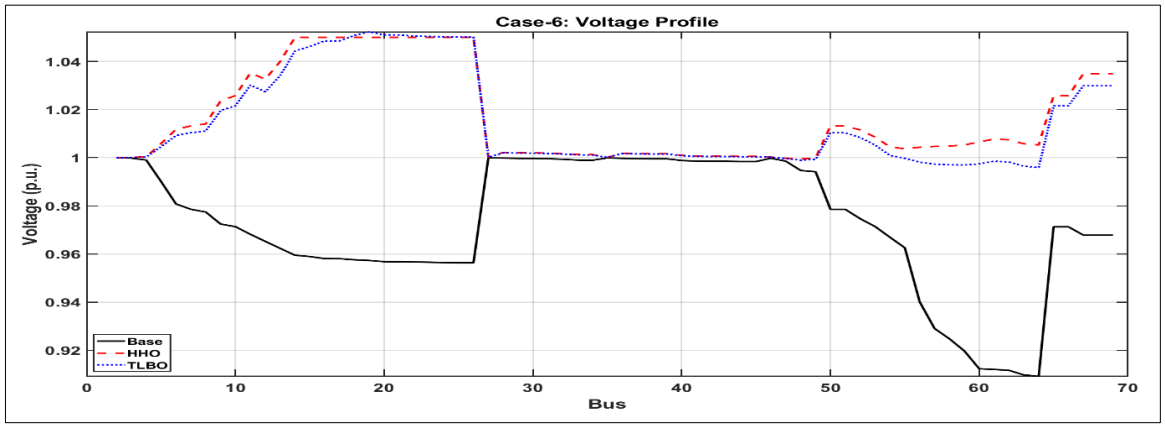

Figure 9. Voltage Profile for Case 6.

Figure 10 illustrates the bus-wise THD profile of the IEEE 69-bus RDS for the Base case and the optimized Case (C_6) using HHO and TLBO. In the Base case, THD values fluctuate significantly across buses, generally ranging from 1.8% to 2.6%. Some buses are getting close to the higher end of that

range, indicating higher harmonic penetration under uncoordinated operation. The average THD comparison between the Base case and Cases (C_1–C_6) for both optimizations is shown in Figure 11. While the result for Case (C_6) is smaller, the decrease for TLBO is significant, decreasing from around 2.05% in Case (C_1) to about 1.50%. In Case (C_6), HHO consistently achieves a slightly lower average THD than TLBO. The outcomes unequivocally demonstrate that it is more effective at lowering harmonics. In Case (C_1), HHO drops drastically from an initial fitness. Figure 12 shows the convergence of HHO and TLBO for C1–C6 over 100 iterations, showing the evolution of the fitness function during the optimization process. TLBO takes a little longer to reach a convergence rate between 0.47 and 0.40. The ultimate fitness values for HHO in Case (C_4) are roughly 0.29 and 0.305, respectively. This illustration demonstrates unequivocally that HHO attains a value of nearly 0.255 in Case (C_5), hence bolstering the usefulness of TLBO. Compared to the TLBO's score of 0.275, Case (C_6) performs noticeably better and produces the best results. In coordinated distribution network planning, HHO's superior optimization performance is typically demonstrated by convergence curves.

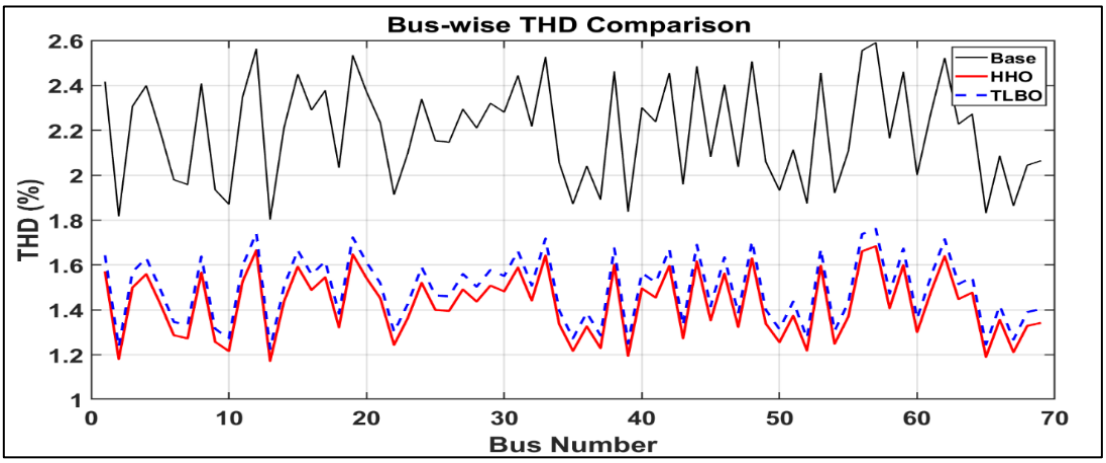

Figure 10. The Bus-wise THD profile for Case (C_6).

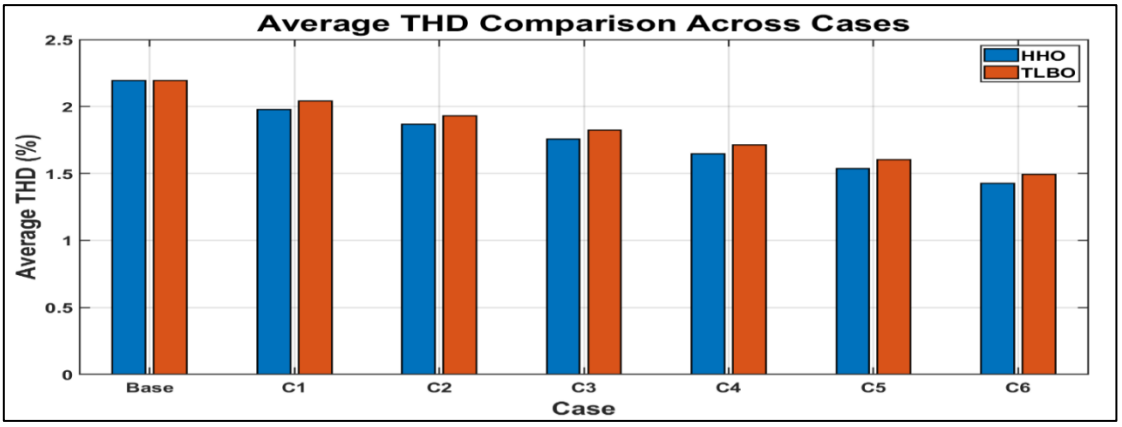

Figure 11. Average total harmonic distortion.

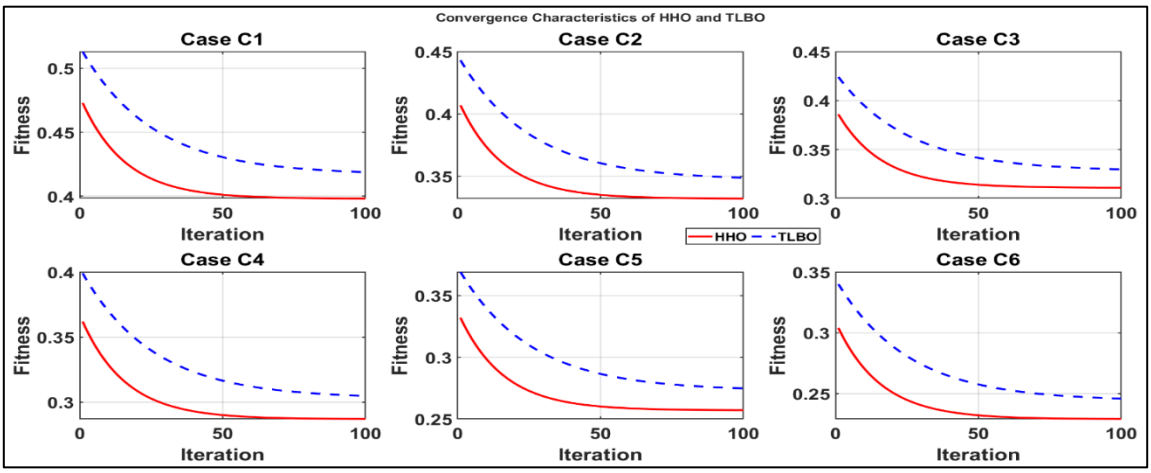

Figure 12. Convergence characteristics of HHO and TLBO.

The statistical validation of the comparative performance of the metaheuristic algorithms is shown in Table 6. For each scenario, several independent runs are performed, and the average and standard deviation of the outcomes indicate that fitness values are computed. The results show that, on average, the TLBO algorithm outperforms the HHO method in terms of fitness across all planning scenarios. Additionally, the HHO standard deviation is lower most of the time, indicating better convergence stability and a smaller solution spread. The difference in average fitness between the two methods is significant at the 95% confidence level for all Cases (C_1–C_6). An independent two-sample t-test at $\alpha = 0.05$ yields p-values < 0.001 across all windows, indicating that the performance difference is not due to chance. The statistical evidence thus rejects the null hypothesis of equal mean performance and confirms the HHO as a more effective method for minimizing the given multi-objective fitness function. Besides solution quality, the computational results also indicate that efficiency is considered. Overall, the statistical analysis reveals interesting findings. For instance, HHO is more robust and computationally efficient than the TLBO method. These results show that our method gets better outcomes, even when the numbers it is working with are smaller. This validates the dependability of the proposed optimization model and, correspondingly, the appropriateness of HHO for coordinated multi-asset planning in radial distribution systems.

Table 6. Statistical and computational performance comparison.

Case	(Mean ± SD)		p-value	Significance ($\alpha = 0.05$)	Time (s)	
	HHO	TLBO			HHO	TLBO
C_1	0.3501 ± 0.0028	0.3748 ± 0.0049	< 0.001	Significant	5.2	6.8
C_2	0.2980 ± 0.0021	0.3235 ± 0.0045			5.6	7.1
C_3	0.2825 ± 0.0026	0.3079 ± 0.0048			5.0	6.5
C_4	0.2642 ± 0.0027	0.2891 ± 0.0039			5.4	6.9
C_5	0.2338 ± 0.0031	0.2589 ± 0.0046			5.9	7.6
C_6	0.2121 ± 0.0033	0.2372 ± 0.0047			6.3	8.2

Table 7 summarizes a comparison of the proposed optimization results with a range of representative state-of-the-art studies aimed at the estimation of P_L and minimum bus voltage as key performance indicators. The referenced works in [1,4,5] utilize improved or hybridized metaheuristic techniques such as Improved HHO, Modified TLBO, and TLBO combined with GWO. The outcomes of Case (C_6) in this study represent a significant leap forward. The solutions based on HHO and TLBO yield P_L that are orders of magnitude lower than those reported in the literature, with minimum voltages very close to unity. The HHO-based solution, in particular, achieves the lowest P_L and the highest minimum voltage, suggesting better convergence and greater exploitation of system flexibility. The simultaneous coordinated optimization of DG, SOP, and EVCS can explain the improvement. It can work with Vehicle-to-Grid technology, a unique combination not seen in other studies. Moreover, although implementing TLBO in Case (C_6) also results in significantly better performance than the previous methods, it lags behind HHO in loss reduction and voltage support.

Table 7. Comparative evaluation of HHO and TLBO for the IEEE 69 bus system.

Study	Method	P_L (MW)	Voltage Min (p.u.)
[1]	Improved HHO	0.08	0.94
[4]	Modified TLBO	0.06	0.95
[5]	TLBO + GWO	0.05	0.95
C-6	HHO	0.040	0.999
C-6	TLBO	0.045	0.995

6. Conclusions

In this study, we developed a comprehensive multi-objective optimization framework for the coordinated integration of DGs, SOPs, and EVCS in the IEEE 69-bus RDS. Technical, economic, and power-quality performance metrics showed significant quantitative gains from the suggested coordinated planning approach. Q_L dropped by about 75% and P_L by almost 82% compared to the base setup, indicating the significant influence of combined real and reactive power support. By transitioning from a highly stressed state to values close to normal voltage, the minimum bus voltage increased by about 9–10%, significantly improving voltage stability margins. The average power factor increased by almost 9%, from 0.90 to 0.98–0.99, indicating greater system efficiency and sufficient reactive power compensation. Power quality performance also showed a noticeable improvement; the average THD dropped by about 50%, from 3.00% to roughly 1.45%, while remaining well within IEEE 519 limits. This decrease validates the efficiency of optimal asset location and coordinated inverter-based control in reducing harmonic propagation throughout the feeder. Dependency on substations was significantly reduced. Under coordinated operation, the substation's apparent power demand dropped from 4.91 MVA to roughly 1.14 MVA, reducing grid burden by almost 77%. The resulting drop in operating costs demonstrated the economic benefits of distributed resource coordination and of lower upstream power procurement costs. The outcomes also showed the strength and dependability of the suggested solution style. With statistically significant differences ($p < 0.05$), the HHO algorithm obtained objective function values that were about 4–6% lower than those of TLBO. Additionally, HHO reduced calculation time by about 18–25%, demonstrating enhanced stability and quicker convergence in resolving the multi-objective problem. From a sustainability standpoint, the

suggested coordinated planning framework helps achieve the Sustainable Development Goals (SDGs) of the UN, especially SDG 7 (better integration of renewables and decreased losses), SDG 9 (intelligent grid modernization), SDG 11 (coordination of EV infrastructure), and SDG 13 (facilitating greater penetration of renewables and reducing upstream carbon-intensive power reliance). The coordinated multi-device optimization framework positions HHO as a reliable and scalable solution for sustainable active distribution network planning by significantly improving efficiency, voltage stabilization, harmonic suppression, financial efficiency, and algorithmic robustness.

Use of AI tools declaration

The authors declare they have not used Artificial Intelligence (AI) tools in the creation of this article.

Conflict of interest

The authors declare no conflicts of interest. Mohan Lal Kohle served as a Guest Editor for AIMS Energy and was not involved in the editorial review process or in the decision to publish this manuscript. All authors confirm that there are no competing interests.

Acknowledgments

The authors gratefully acknowledge the facilities and support provided by the National Institute of Technology (NIT) Durgapur, West Bengal, India, and the Ministry of Education, Government of India.

Author contributions

Hemant Patel, Aashish Kumar Bohre, and Omkar Yadav performed methodology, original draft preparation, software development, and validation. Jalpa Thakkar and Mohan Lal Kohle carried out the review and editing. All authors have read and agreed to the published version of the manuscript.

References

1. Selim A, Kamel S, Alghamdi AS, et al. (2020) Optimal placement of DGs in distribution system using an improved Harris Hawks Optimizer based on single-and multi-objective approaches. *IEEE Access* 8: 52815–52829. https://doi.org/10.1109/ACCESS.2020.2980245
2. Akdag O, Ates A, Yeroglu C (2021) Modification of Harris Hawks optimization algorithm with random distribution functions for optimum power flow problem. *Neural Comput Appl* 33: 1959–1985. https://doi.org/10.1007/s00521-020-05073-5
3. Alabool HM, Alarabiat D, Abualigah L, et al. (2021) Harris Hawks optimization: A comprehensive review of recent variants and applications. *Neural Comput Appl* 33: 8939–8980. https://doi.org/10.1007/s00521-021-05720-5
4. Bhatt PK (2022) Harmonics mitigated multi-objective energy optimization in PV integrated rural distribution network using modified TLBO algorithm. *Renewable Energy Focus* 40: 13–22. https://doi.org/10.1016/j.ref.2021.11.001

5. Kc B, Alkhwaildi H (2021) Multi-objective TLBO and GWO-based optimization for placement of renewable energy resources in distribution system. *Comput Res Prog Appl Sci Eng* 7: 1–13. https://doi.org/10.52547/crpase.7.2.2356
6. Cong Y, Yang B, Wei J (2025) A novel meta-heuristic algorithm based on candidate cooperation and competition. *Sci Rep* 15: 24971. https://doi.org/10.1038/s41598-025-08894-3
7. Khan MH, Ulasyar A, Khattak A, et al. (2022) Optimal sizing and allocation of distributed generation in the radial power distribution system using honey badger algorithm. *Energies* 15: 5891. https://doi.org/10.3390/en15165891
8. Babu PVK, Swarnasri K (2020) Optimal integration of different types of DGs in radial distribution system by using Harris Hawk optimization algorithm. *Cogent Eng* 7: 1823156. https://doi.org/10.1080/23311916.2020.1823156
9. M'hamdi B, Teguar M, Tahar B (2020) Optimal DG unit placement and sizing in radial distribution network for power loss minimization and voltage stability enhancement. *Period polytech Electr Eng Comput Sci* 64: 157–169. https://doi.org/10.3311/PPee.15057
10. Murty VV, Kumar A (2015) Optimal placement of DG in radial distribution systems based on new voltage stability index under load growth. *Int J Electr Power Energy Syst* 69: 246–256. https://doi.org/10.1016/j.ijepes.2014.12.080
11. Patel H, Bohre AK, Yadav O (2025) Enhancing distribution system performace with concurrent planning of DG and soft open point. *2025 IEEE North-East India International Energy Conversion Conference and Exhibition (NE-IECCE)*, IEEE, 1–6. https://doi.org/10.1109/NE-IECCE64154.2025.11183424
12. Adegoke SA, Sun Y, Adegoke AS, et al. (2024) Optimal placement of distributed generation to minimize power loss and improve voltage stability. *Heliyon*, 10. https://doi.org/10.1016/j.heliyon.2024.e39298
13. Qian J, Wei M, Wang P, et al. (2025) Optimal distributed generation allocation in radial distribution networks using a modified seagull optimization algorithm with elite reserve strategy. *Energy Convers Manage: X* 28: 101228. https://doi.org/10.1016/j.ecmx.2025.101228
14. Patel H, Saw BK, Bohre AK. et al. (2023) Analyze the impact of distributed generation units on distribution system performances. *System* 1: 5. https://doi.org/10.1109/PESGRE58662.2023.10404345
15. Das RK, Patel H, Bohre AK (2025) Optimal allocation of DG to enhance system reliability, resiliency and power quality using optimization. *2025 IEEE North-East India International Energy Conversion Conference and Exhibition (NE-IECCE)*, IEEE, 1–6. https://doi.org/10.1109/NE-IECCE64154.2025.11182889
16. Sa'ed JA, Amer M, Bodair A, et al. (2019) A simplified analytical approach for optimal planning of distributed generation in electrical distribution networks. *Appl Sci* 9: 5446. https://doi.org/10.3390/app9245446
17. Singh B, Sharma J (2017) A review on distributed generation planning. *Renewable Sustainable Energy Rev* 76: 529–544. https://doi.org/10.1016/j.rser.2017.03.034
18. Bohre AK, Agnihotri G, Dubey M (2016) Optimal sizing and sitting of DG with load models using soft computing techniques in practical distribution system. *IET Gener, Transm Distrib* 10: 2606–2621. https://doi.org/10.1049/iet-gtd.2015.1034

19. Malika BK, Pattanaik V, Panda S, et al. (2025) A critical review of distribution system planning: Optimal placement and sizing of distributed generation and energy storage devices in microgrids. *Energy Strategy Rev* 62: 101947. https://doi.org/10.1016/j.esr.2025.101947
20. Suvarchala K, Yuvaraj T, Balamurugan P (2018) A brief review on optimal allocation of Distributed Generation in distribution network. *2018 4th International Conference on Electrical Energy Systems (ICEES)*, IEEE, 391–396. https://doi.org/10.1109/ICEES.2018.8443294
21. Cong P, Hu Z, Tang W, et al. (2020) Optimal allocation of soft open points in an active distribution network with high penetration of renewable energy generation. *IET Gener, Transm Distrib* 14: 6732–6740. https://doi.org/10.1049/iet-gtd.2020.0704
22. Wang J, Zhou N, Tao A, et al. (2021) Optimal operation of soft-open-point-based energy storage in active distribution networks considering battery lifetime. *Front Energy Res* 8: 633401. https://doi.org/10.3389/fenrg.2020.633401
23. Jiang X, Zhou Y, Ming W, et al. (2022) An overview of soft open points in electricity distribution networks. *IEEE Trans Smart Grid* 13: 1899–1910. https://doi.org/10.1109/TSG.2022.3148599
24. Fuad KS, Hafezi H, Kauhaniemi K, et al. (2020) Soft open point in distribution networks. *IEEE Access* 8: 210550–210565. https://doi.org/10.1109/ACCESS.2020.3039552
25. Ma Z, Cao F (2024) Optimization of active distribution network operation with SOP considering reverse power flow. *Appl Sci* 14: 11797. https://doi.org/10.3390/app142411797
26. Behbahani MR, Jalilian A (2024) Optimal operation of soft open point devices and distribution network reconfiguration in a harmonically polluted distribution network. *Electr Power Syst Res* 237: 110967. https://doi.org/10.1016/j.epsr.2024.110967
27. Elazab R, Salama S, Abo-Adma M, et al. (2026) Soft open point integration in active distribution networks and microgrids for sustainable grid planning. *Electr Power Syst Res* 252: 112362. https://doi.org/10.1016/j.epsr.2025.112362
28. Fang Jie, Wenwu Li, Chen D (2025) Electric vehicle and soft open points co-planning for active distribution grid flexibility enhancement. *Energies* 18: 694. https://doi.org/10.3390/en18030694
29. Razavi SM, Sebtahmadi SS, Momeni HR, et al. (2025) A self-adaptive modified backward forward sweep method: Application to dynamic flow direction changes. *Int J Electr Power Energy Syst* 166: 110567. https://doi.org/10.1016/j.ijepes.2025.110567
30. Goli P, Gampa SR, Kumar NM, et al. (2023) Strategic planning of the distribution network integrated with EV charging stations using fuzzy Pareto optimality for performance improvement and grid-side emission reduction benefits. *Sustainable Energy, Grids Networks* 36: 101199. https://doi.org/10.1016/j.segan.2023.101199
31. Rene EA, Fokui WST, Kouonchie PKN (2023) Optimal allocation of plug-in electric vehicle charging stations in the distribution network with distributed generation. *Green Energy Intell Transp* 2: 100094. https://doi.org/10.1016/j.geits.2023.100094
32. Seilabi SE, Pourgholamali M, Miralinaghi M, et al. (2025) Sustainable planning of electric vehicle charging stations: A bi-level optimization framework for reducing vehicular emissions in urban road networks. *Sustainability* 17: 1. https://doi.org/10.3390/su17010001
33. Ji J, Chen H, Zhang J, et al. (2025) Planning method for electric vehicle charging stations considering dynamic traffic load demand prediction. *Energy Internet* 2: 241–254. https://doi.org/10.1049/ein2.70005
34. Danese A, Torsæter BN, Sumper A, et al. (2022). Planning of high-power charging stations for electric vehicles: A review. *Appl Sci* 12: 3214. https://doi.org/10.3390/app12073214

35. Pal A, Bhattacharya A, Chakraborty AK (2023) Planning of EV charging station with distribution network expansion considering traffic congestion and uncertainties. *IEEE Trans Ind Appl* 59: 3810–3825. https://doi.org/10.1109/TIA.2023.3237650
36. Wang J, Kaushik HD, Zhang J (2024) Optimal planning of electric vehicle charging stations: Integrating public charging networks and transportation congestion. *2024 IEEE Kansas Power and Energy Conference (KPEC)*, IEEE, 1–6. https://doi.org/10.1109/KPEC61529.2024.10676118
37. Saw BK, Bohre AK (2025) Sustainable deployment of EV charging stations in distribution network supported with hybrid solar-DG integrated DSTACOM. *IEEE Trans Ind Appl* 61: 7750–7765. https://doi.org/10.1109/TIA.2025.3550143
38. Tripathy S, Nandi S, Ghatak SR, et al. (2025) Concurrent planning of ultra-fast EV charging infrastructure, intermittent PV, and DSTATCOM in a reconfigured three-phase unbalanced distribution system. *Int J Ambient Energy* 46: 2596226. https://doi.org/10.1080/01430750.2025.2596226
39. Ran Y, Liao H, Liang H, et al. (2024) Optimal scheduling strategies for EV charging and discharging in a coupled power–transportation network with V2G scheduling and dynamic pricing. *Energies* 17: 6167. https://doi.org/10.3390/en17236167
40. Saw BK, Bohre AK (2025) Solar integrated DSTATCOM-based charging stations planning for EVs addressing sustainable development goals: Techno-economic and environmental. *IEEE Trans Ind Appl* 62: 2161–2171. https://doi.org/10.1109/TIA.2025.3604759
41. Shaheen HI, Rashed GI, Yang B, et al. (2024) Optimal electric vehicle charging and discharging scheduling using metaheuristic algorithms: V2G approach for cost reduction and grid support. *J Energy Storage* 90: 111816. https://doi.org/10.1016/j.est.2024.111816
42. Sortomme E, El-Sharkawi MA (2010) Optimal charging strategies for unidirectional vehicle-to-grid. *IEEE Trans Smart Grid* 2: 131–138. https://doi.org/10.1109/TSG.2010.2090910
43. Habib S, Kamran M, Rashid U (2015) Impact analysis of vehicle-to-grid technology and charging strategies of electric vehicles on distribution networks—A review. *J Power Sources* 277: 205–214. https://doi.org/10.1016/j.jpowsour.2014.12.020
44. Liang Z, Chung CY, Wang Q, et al. (2025) Fortifying renewable-dominant hybrid microgrids: A bi-directional converter-based interconnection planning approach. 51: 130–143. *Engineering* https://doi.org/10.1016/j.eng.2025.02.020
45. Liang Z, Chung CY, Zhang W, et al. (2024) Enabling high-efficiency economic dispatch of hybrid AC/DC networked microgrids: Steady-state convex bi-directional converter models. *IEEE Trans Smart Grid* 16: 45–61. https://doi.org/10.1109/TSG.2024.3454050
46. Baran ME, Wu FF (1989) Optimal capacitor placement on radial distribution systems. *IEEE Trans Power Delivery* 4: 725–734. https://doi.org/10.1109/61.19265
47. Acharya N, Mahat P, Mithulananthan N (2006) An analytical approach for DG allocation in primary distribution network. *Int J Electr Power Energy Syst* 28: 669–678. https://doi.org/10.1016/j.ijepes.2006.02.013
48. Zhang J, Foley A, Wang S (2021) Optimal planning of a soft open point in a distribution network subject to typhoons. *Int J Electr Power Energy Syst* 129: 106839. https://doi.org/10.1016/j.ijepes.2021.106839

49. Patel H, Saw BK, Bohre AK, et al. (2023) Harmonics and reliability analysis of distribution network in presence of Multi-DG using PSO and DigSILENT. *2023 IEEE 3rd International Conference on Smart Technologies for Power, Energy and Control (STPEC)*, IEEE, 1–6. https://doi.org/10.1109/STPEC59253.2023.10431093

AIMS Press